Structure and wear mechanisms of nano-structured TiAlCN/VCN multilayer coatings

LUO, Q. <http://orcid.org/0000-0003-4102-2129>, SCHIMPF, C., EHIASARIAN, A. P. <http://orcid.org/0000-0001-6080-3946>, CHEN, L. and HOVSEPIAN, P. <http://orcid.org/0000-0002-1047-0407>

Structure and Wear Mechanisms of Nano-Structured TiAlCN/VCN Multilayer Coatings

Quanshun Luo*, Christian Schimpf, Arutian P. Ehiasarian, Papken Eh. Hovsepian

Materials and Engineering Research Institute, Sheffield Hallam University, Sheffield, S1 1WB, UK.

Summary: Dry sliding wear of transition metal nitride coatings usually results in a dense and strongly adhered tribofilm on the worn surface. This paper presents detailed electron microscopy and Raman spectroscopy characterizations of the microstructure a newly developed multilayer coating TiAlCN/VCN and its worn surface after pin-on-disc sliding wear against an alumina ball. The friction coefficient in a range of 0.38 – 0. 6 was determined to be related to the environment humidity, which resulted in a wear coefficient of the coating varying between 10^{-17} and 10^{-16} $m^3N^{-1}m^{-1}$. TEM observation of worn surfaces showed that, when carbon was incorporated in the nitride coating, the formation of dense tribofilm is inhibited.

Key words: Tribology; Transmission electron microscopy (TEM); Raman spectroscopy; Physical vapour deposition (PVD); Nanolayers; Nitrides

Introduction

Nano-structured multilayer TiAlN/VN coatings of high hardness and good adhesion property have been grown by the combined cathodic arc and unbalanced magnetron reactive sputter deposition since 2000 [1]. The TiAlN/VN coatings have shown both low friction coefficient and extremely low wear rate in un-lubricated sliding wear as compared to other transition metal nitride coatings. This is attributed to the formation of a nanometer-scale, amorphous and multicomponent Ti-Al-V-O oxide film [2]. The tribofilm is strongly adhered to the parent nitride surface. It therefore dominates the low-friction property and protects the surface from mechanical wear. In industrial trials of coolant-free high-speed milling aluminium alloys, TiAlN/VN coated tools show low cutting forces, long lifetime and significantly reduced built-up edge (BUE) formation as compared to the uncoated tools or those coated with other TiAlN based coating [3]. In the same application area, the performance of carbon-based coatings such as diamond and diamond-like carbon are widely acknowledged for their low affinity to aluminium which brings about an almost BUE-free cutting process [4].

When carbon was introduced in the deposition of TiAlCN/VCN multilayer coatings in a reactive atmosphere of nitrogen and methane [5], beneficial effects have been found in the tribological properties and tool performance [6]. This is obviously related to the modification of wear mechanisms especially the behaviour of tribofilm formation. It has been reported in literatures that tribofilm formation can be interrupted by the presence of surface active species [7] and that carbon implantation in the TiN coating leads to a significant reduction of friction coefficient [8]. The results presented in this paper are concentrated on the microstructure and dry-sliding wear mechanisms of the TiAlCN/VCN coatings. Special attention has been paid to the influence of carbon incorporation on the wear failure mechanisms including the generation of tribofilm.

Experimental Part

The TiAlCN/VCN coatings were grown on polished high speed steel coupons by using the combined high power impulse magnetron sputtering / unbalanced magnetron sputtering (HIPIMS/UBM) technology [6]. For this research the arc power supply on one of the cathodes in the Hauzer HTC-100-4 system was replaced by a HIPIMS power supply (Advanced Converters, Poland), which allowed sequential operation in HIPIMS and UBM mode. The advantages of

utilizing the novel HIPIMS surface treatment prior to the coating deposition are the enhanced coating adhesion and very smooth coating surface due to elimination of macroparticle induced defects [9]. After the HIPIMS etching, a 0.4 μm thick TiAlN base layer was deposited followed by 2.6 μm thick TiAlCN/VCN layer deposited by standard UBM process in a mixed N_2 + CH_4 + Ar atmosphere.

Sliding wear tests were conducted by using a computer-programmed CSM ball-on-disc tribometer at conditions: with a 6-mm counterpart ball of alumina, applied load 5 N, sliding speed 0.1 ms^{-1}, room temperature in a range of 20 – 30 ^{0}C. As preliminary tests revealed an effect of relative humidity (RH) on the amplitude of friction coefficient, the sliding tests were performed in a range of RH values from 15 to 75%.

The worn surfaces obtained after each wear test were examined using scanning electron microscopy (SEM), energy dispersive X-ray (EDX) spectroscopy and Raman spectroscopy. The Raman analysis was undertaken on a Renishaw-2000 Raman System with the excitation wavelength of 632.8 nm from a HeNe laser. This system allowed a lower spectral limit of ~150 cm^{-1} and upper limit of 2,000 cm^{-1}.

A Philips STEM-CM20 instrument, operating at 200 kV with a LaB_6 filament, was employed for TEM bright field (BF) and dark field (DF) imaging, selected area diffraction (SAD) analysis and EDX analysis. Longitudinal cross-sectional TEM samples containing the worn surface were prepared following a procedure described in [2]. In addition, wear particles were collected on a 200-mesh carbon-film copper grid for direct TEM analysis.

Results and Discussion

Mechanical and Structural Characterizations

Detailed mechanical properties and structural characterization of the TiAlCN/VCN coatings have been reported in [6]. Typically, the coatings exhibited Knoop hardness $HK_{0.025}$ 27.7 GPa, Young's modulus 296.9 GPa, and critical scratch load 58 N. The hardness and elastic modulus of the TiAlCN/VCN are comparable to those of the carbon-free coating TiAlN/VN. Note that the excellent adhesion property is attributed to the substrate surface etching with the HIPIMS process [9], where the coatings with cathodic arc etched interface showed scratch load of approximately 45 – 50 N.

Fig. 1 shows SEM and TEM characterization of typical TiAlCN/VCN coating. The coating shows columnar grains with rough growth surface and nano-scale grain size. The columnar grains are fully dense where slightly sub-dense area can be seen along the column boundaries. The coatings were determined to have a NaCl-type cubic crystalline structure following a preferred (220) growth orientation. Such structural features are similar to the carbon-free TiAlN/VN coatings grown under the same bias voltage (-75V) [2, 10].

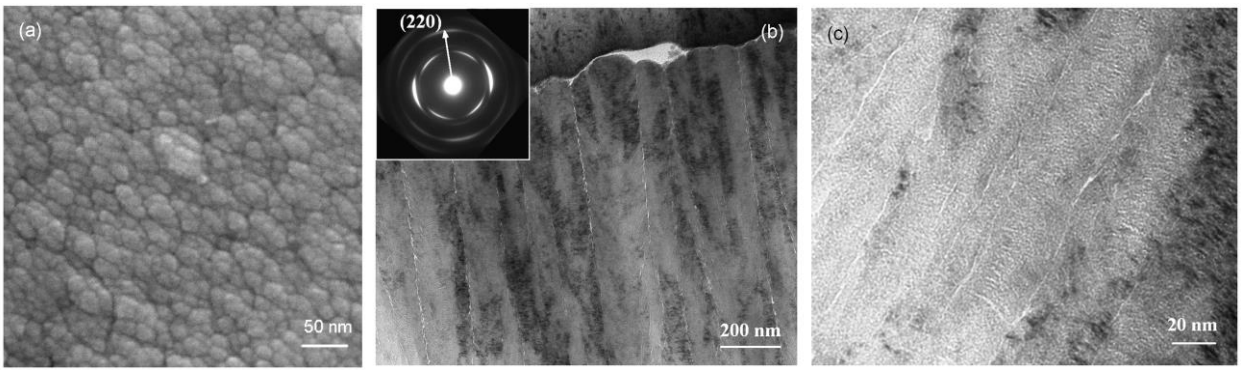

Figure 1. Electron microscopy of TiAlCN/VCN coatings. (a) High-resolution SEM showing the coating surface containing feature of nanoscale grain size. (b) Cross-section TEM BF image

showing dense columnar morphology, with a SAD insert showing the cubic crystalline structure and (220) texture. (c) Cross-sectional TEM BF image at higher magnification showing the irregular multilayer morphology.

Raman spectroscopy analysis confirmed the predominant structure of nitride in the TiAlCN/VCN, seeing the acoustic and optical bands of cubic nitride (at 250 and 650 cm^{-1} respectively) in spectra (a – c) in Fig. 2. However, the optical band is lower as compared to the carbon-free TiAlN/VN whereas the intensity of the acoustic bands is comparable. The lower optical band can be explained by the fill-up of some nitrogen vacancies with carbon atoms. Moreover, the Raman spectra acquired in the TiAlCN/VCN coatings showed, although with low intensity in spectrum (b), the disordered (D) and graphite (G) bands of carbon structure. The existence of small amount of amorphous carbon was also indicated in the modified TiAlCN/VCN multilayer fringes in high-magnification de-focused bright field imaging as compared to TiAlN/VN [6, 10].

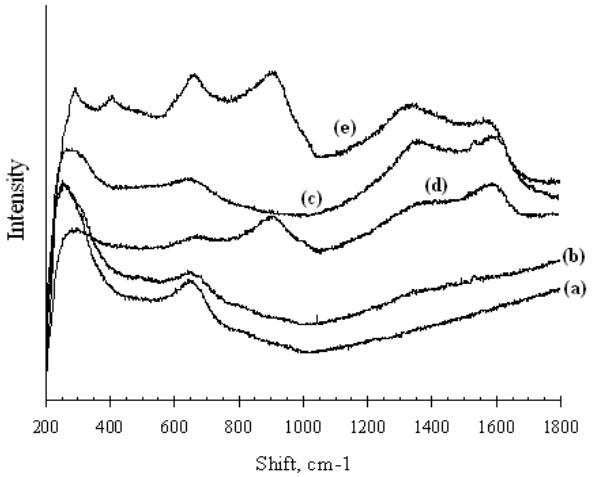

Figure 2. A collection of Raman spectra obtained in: (a) TiAlN/VN coating; (b) TiAlCN/VCN coating at CH_4:N_2 = 1:2; (c) TiAlCN/VCN coating at CH_4:N_2 = 1:2; (d) Wear debris attached inside the wear track; and (e) loose wear debris dropped on a glass plate.

Tribological Properties

Table 1 shows typical friction and wear behaviour of TiAlCN/VCN coatings tested at a range of environment humidity. At low humidity (RH 18 %), the coating exhibited an average friction coefficient 0.59 leading to a wear coefficient of 4.1×10^{-16} $m^3N^{-1}m^{-1}$. When tested at higher humidity (RH 30 – 75%), the obtained friction coefficient was as low as 0.38 leading to significantly lower coefficient typically in the order of 10^{-17} $m^3N^{-1}m^{-1}$. The results suggest environment dependent friction and wear properties of the carbon containing coating whereas good lubrication behaviour exists at higher humidity. This behaviour is similar to carbon-based materials. For example, in DLC coatings, high levels of sp^2-bonding in graphite and DLC films leads to high friction. These bonds are greatly weakened by the presence of water molecules leading to lower friction [11, 12]. It is, however, dissimilar to the carbon-free nitride coatings according to our experiments. Under the same range of test conditions, pure nitride coatings TiAlN/VN and TiAlCrYN showed the friction and wear behaviours being independent of the variation of relative humidity.

Table 1 Friction and wear properties of TiAlCN/VCN coating.

	RH %	Coefficient of friction	Coefficient of wear 10^{-17} $m^3N^{-1}m^{-1}$
Test 1	18	0.59	41.0
Test 2	33	0.38	4.1
Test 3	70	0.42	2.5

Characterizations of Worn Surfaces and Wear Debris

The wear track obtained in each wear test contained islands of wear debris agglomerates distributing over the smooth worn surface and loose wear debris dispersing along the wear track boundaries. Preliminary SEM-EDX analysis revealed that the wear debris contained substantial amount of oxygen and the smooth worn surface area was free of oxygen.

Typical Roman spectra of wear products have been shown in Fig. 2 excluding the spectrum of smooth worn surface which was the same as the as-deposited coating. Spectrum (d) shows a broad peak at 800 – 1000 cm^{-1} and strong D-G bands, indicating a mixture of complex oxides and carbon. The shift bands at 250 cm^{-1} and 650 cm^{-1} were contributions from the surrounding TiAlCN/VCN coating. To avoid the interference, some loose debris were taken away from the wear track and placed on a clean glass plate. The obtained spectrum is shown in spectrum (e), which shows shift bands at 299.1, 416.4, 505.0, 625.11, 672.8, 913.0, 1344.7, and 1580.2 cm^{-1}. The spectrum may contain contributions from carbon structure (the D-G bands at 1356 and 1592 cm^{-2} respectively) and several oxides, including V_2O_5 (shift bands at 280, 400, 480, 520 and 1000 cm^{-1}), Al_2O_3 (shift bands at 418, 639, 873, 993 and 1400 cm^{-1}) and TiO_2 (shift bands at 395, 639 and 792 cm^{-1}) [14, 15]. In some wear debris areas, however, the D-G bands were not shown, indicating non-homogeneous distribution of carbon. In brief, Raman spectroscopy analysis suggested that the wear debris contains a mixture of several oxides and amorphous carbon.

TEM imaging of longitudinal cross-sections of worn surface samples revealed that, there was no tribofilm closely attached on the TiAlCN/VCN worn surface, Figs. 3a-b. Instead, there were only areas where loose agglomerates of wear debris were left on the top edge, Fig. 3b. This phenomenon was repeatedly observed in all the imaged areas. In some areas, TEM observation has shown cracks and delamination sheets, Fig. 3a. The fact that no tribofilm was formed on the TiAlCN/VCN worn surface formed a striking contrast to the cases of carbon-free nitride coatings like TiAlN/VN [2] and TiAlN/CrN [13] in which a dense tribofilm was found to closely adhere to the parent worn surface.

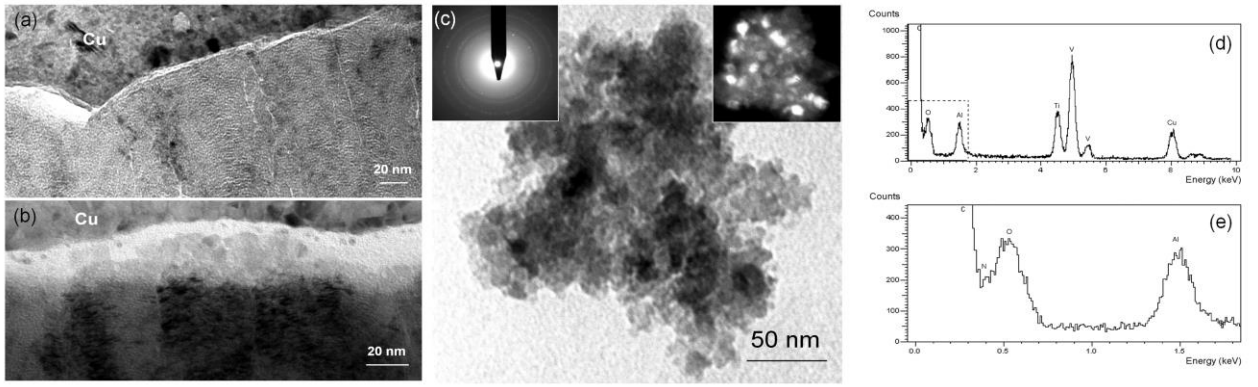

Figure 3. Analytical TEM analysis of TiAlCN/VCN and wear debris. (a-b) cross-sectional bright field images showing no tribofilm but loose agglomerates of wear debris on the worn surface top. (c) A bright field image showing wear debris exhibiting an amorphous matrix containing nitride nano-particles (seeing the inserts of associated electron diffraction patters and dark field image). (d) An EDX spectrum of wear debris with the highlighted low-energy area shown in (e).

Fig. 3c shows TEM analyses of loose wear debris. The main bright field micrograph shows an amorphous medium containing nanometer scale crystalline particles. Electron diffraction pattern of the imaged area indicated a NaCl-type cubic structure of the particles, which was further confirmed by the associated dark field imaging. These particles resulted from mechanical wear of the coating. TEM-EDX analysis in Fig. 3d-e show substantial amount of oxygen together with the presence of Al, Ti and V, which was consistent to the SEM-EDX results as described before. Therefore, the wear of the TiAlCN/VCN coatings was classified as oxidation wear and mechanical wear. The

oxidation wear was consistent to those previously found in the sliding wear of TiAlN/VN. the mechanical wear could have occurred in the running-in period of sliding by high-stress and adhesive breaking [16] and might also be a result of delamination wear like those observed in other transition metal nitride coatings [13, 17].

Effect of Carbon in the Tribofilm Formation

As a general phenomenon of dry sliding wear, tribofilms were observed on the worn surfaces of several ceramics and transition metal nitride coatings. In literature [7], the generation of tribofilm was discussed concerning its bonding forces as well as the inhibition of tribofilm. The bonding forces for tribofilm formation were reported to be mainly van de Waals forces as well as electrostatic forces which are strong enough to resist being wiped off by the slider. On the other hand, any surface active specie on the sliding surface such as lubricant may reduce the interactive interaction and may lead to the inhibition of tribofilm. In transition nitride coatings such as TiN, the incorporation of carbon has been widely to have significant mechanical and tribological properties. For example, when a carbon-implanted TiN was tested in dry sliding conditions against a soft austenite stainless steel, it exhibited lower friction and lower wear rate than the carbon-free TiN [8]. A major difference in wear mechanisms between the TiN and the carbon-implanted TiN was that, the latter showed significantly reduced adhesive wear.

In the TiAlCN/VCN coatings studied, carbon has been found to exist both in the as-deposited coating and in the resultant wear debris according to our Raman spectroscopy study (Fig. 2). Despite a similar predominant wear mechanism of tribo-oxidation occurring in the carbon-containing TiAlCN/VCN (Figs. 2-3) and the carbon-free TiAlN/VN (refs. [2, 15]), the existence of carbon phase in the wear debris indicated its possible influence on the agglomeration of wear debris and the adhesive interaction between wear debris and the worn surface. According to our TEM observations, the carbon-containing TiAlCN/VCN coatings showed no tribofilm on the dry-sliding worn surfaces, being strikingly different to those carbon-free nitrides such as TiAlN/VN and TiAlCrYN where a closely attached tribofilm was generated under the same sliding conditions as described in this paper. The inhibition of tribofilm reveals significantly reduced adhesive interaction of the TiAlN/VN with the attached oxide debris.

Conclusions

1. The TiAlCN/VCN coatings grown by the combined HIPIMS/UBM technology exhibited predominantly a NaCl-type cubic crystalline structure whereas carbon exists partly in the crystalline structure and partly as amorphous carbon.
2. In dry sliding wear tests, the TiAlCN/VCN coatings showed both low friction coefficient ($\mu = 0.4$) and low wear rate ($Kc = \sim 10^{-17}$ $m^3N^{-1}m^{-1}$) in a range of relative humidity RH = 23 – 70%. The formation of adhesive tribofilm was inhibited, whereas the predominant wear mechanism was tribo-oxidation.

References

[1] W. D. Münz, L. A. Donohue, P. Eh. Hovsepian, Surf. Coat. Technol. 2000, 125, 269.

[2] Q. Luo, P. Eh. Hovsepian, Thin Solid Films, 2006, 497, 203.

[3] Q. Luo, G. Robinson, M. Pittman, M. Howarth, W. –M. Sim, M. R. Stalley, H. Leitner, R. Ebner, D. Caliskanoglu, P. Eh. Hovsepian, Surf. Coat. Technol. 2005, 200, 123.

[4] M. Lahres, P. Müller-Hummel, O. Doerfel, Surf. Coat. Technol. 1997, 91, 116.

[5] P. Eh. Hovsepian, A. P. Ehiasarian, T. Deeming, PVD coated substrate, Pat. Appl. B0508485.0 filed 27 Apr. 2005.

[6] P. Eh. Hovsepian, A. P. Ehiasarian, T. Deeming, C. Schimpf, Novel TiAlCN/VCN nanoscale multilayer PVD coatings deposited by the combined high power impulse magnetron sputtering / unbalanced magnetron sputtering (HIPIMS/UBM) technology, Thin Solid Films, submitted, 2006.

[7] O. O. Ajayi, K. C. Ludema, Wear, 1990, 140, 191.

[8] T. Jamal, R. Nimmagadda, R. F. Bunshah, Thin Solid Films 1980, 73, 245.

[9] A. P. Ehiasarian, J. G. Wen, I. Petrov, Interface microstructure engineering by high power impulse magnetron sputtering for the enhancement of adhesion, J. Appl. Phys. 2006, submitted.

[10] Q. Luo, D. B. Lewis, P. Eh. Hovsepian, W. D. Münz, J. Mater. Res. 2004, 19, 1093.

[11] A. Erdemir, Tribol. Inter. 2004, 37, 1005.

[12] C. Donnet, M. Belin, J. C. Augé, J. M. Martin, A. Grill, V. Patel, Surf. Coat. Technol. 1994, 68-69, 626.

[13] Q. Luo, W.M. Rainforth, W.-D. Münz, Scr. Mater. 2001, 45, 399.

[14] H. C. Barshilia, K. S. Rajam, J. Mater. Res. 2004, 19, 3196.

[15] C. P. Constable, J. Yarwood, P. Eh. Hovsepian, L. A. Donohue, D. B. Lewis, W.-D. Münz, J. Vac. Sci. Technol. 2000, A18, 1681.

[16] S. K. Biswas, Wear 2000, 245, 178.

[17] Q. Luo, W. M. Rainforth, W. –D. Münz, Wear 1999, 225-229, 74.